Proceedings of the 16th International Conference on Soil Mechanics and Geotechnical Engineering

doi:10.3233/978-1-61499-656-9-1913

Effect of water composition on rockfill compressibility

Effet de composition de l'eau sur la compressibilité des enrochements

E. Romero, E.E. Alonso & O. Hueso
Department of Geotechnical Engineering and Geosciences, Universitat Politècnica de Catalunya, Barcelona, Spain

ABSTRACT

The paper presents results of oedometer tests on a rockfill-type material aimed at studying the effect of water composition on material deformational response. Flooding tests with different liquids and pore fluid replacement tests were performed at constant vertical stress. Splitting tensile strength tests were also performed to relate the micromechanics of particle fracture to the observed deformational behavior. Osmotic suction was used as the relevant variable to measure and control the influence of the liquid action.

RÉSUMÉ

L'article présente les résultats d'essais oedométriques sur un matériau d'enrochement dans le but d'étudier l'effet de la composition de l'eau sur la réponse en déformation du matériau. Des essais de mouillage avec différents liquides ainsi que des tests ou le fluide interstitiel est remplacé, ont été réalisés à contrainte verticale constante. Des essais de résistance à la traction ont de plus été faits pour relier la micromécanique de la fracture des agrégats au comportement observé en déformation.

1 INTRODUCTION

Rockfill mechanical behavior is very sensitive to the action of water, which is of particular concern during the design and the performance stage of rockfill and zoned dams. Breakage of rock particles and crack propagation are the main micromechanical phenomena behind the explanation of the macrostructural collapse and the increase of compressibility on wetting, as recently suggested by Oldecop & Alonso (2001), Chávez & Alonso (2003) and Oldecop & Alonso (2003) on the basis of controlled-suction tests. Particle breakage in rockfill-type material mainly depends on the strength of individual particles, the grain size distribution, the stress level and the relative humidity prevailing at the rockfill voids. This last factor, associated with the action of water, explains the collapse observed when the material undergoes total or partial wetting at constant stress. Water action due to vapor transfer has been usually assessed by its potential or total suction, which is a magnitude linked by the psychrometric law to the relative humidity of the air surrounding the rock particles (Coussy, 1995).

However, crack propagation also depends on the chemical action of the liquid contained within the rock particles. This paper specifically explores this phenomenon, focusing on the macroscopic deformational behavior of a rockfill, when the material is imbibed with liquids of different composition or when the initial pore liquid is replaced by a liquid with a different composition. An experimental programme under oedometer conditions was envisaged on a quartzitic slate with the aim of getting a better understanding of rockfill macroscopic deformation mechanisms. Total suction, which is equivalent to the osmotic component under a matric suction equal to zero on saturation, was again used as the relevant variable to measure and control the influence of the liquid action on the mechanical behavior. Data from splitting tensile strength tests (diametral compression tests on quasi-spherical particles between flat platens) were also obtained with different imbibition liquids and used to relate the micromechanics of grain fracture to the deformational behavior observed at macroscopic scale.

2 EXPERIMENTAL PROGRAMME

A series of oedometer tests on a rockfill-type material were performed to investigate the effects of water composition on rockfill compressibility and collapsibility. The tested material was a statically compacted crushed slate from the Pancrudo River outcrop (Aragón, Spain). The granulometric and engineering properties of the material are summarized in Table 1.

Table 1. Properties of the material (Oldecop & Alonso 2001, Chávez 2003).

Property	Value (range)
D_{max}, D_{60}, D_{30}, D_{10}, D_{min} (granulometry)	20.0, 11.4, 7.8, 4.3, 0.4 mm
Flakiness index (EN 933-3)	19 - 39%
Solid density (ASTM C97-90)	2.75 Mg/m^3
Particle porosity	6.3 – 11.8%
Water absorption (ASTM C97-90)	1.36 – 1.87%
Uniaxial compression strength (ASTM D2938-86)	14.2 – 31.9 MPa
Tensile strength (ASTM D3967-86)	0.6 – 1.4 MPa

The oedometer test programme was performed in a stress-controlled oedometer cell with 150 mm in diameter and 70 mm high. Specimen compaction was carried out statically in one layer and directly in the oedometer ring at a maximum vertical stress of 2.4 MPa. The dry density reached after compaction was around 1.75 Mg/m^3, which was slightly lower than the dry density 1.77 Mg/m^3 achieved in the standard Proctor test (Oldecop & Alonso, 2001). The particle size distribution of the as-compacted material is plotted in Figure 5.

The first stage of the test programme included loading and unloading paths with sample flooding at two vertical stresses: 0.9 and 1.8 MPa. The samples equilibrated at hygroscopic humidity (relative humidity of around 50% and associated with a total suction of 100 MPa) were loaded in steps to the target flooding stress level (path AB in Figure 1), then soaked with different liquids (path BC in Figure 1), and further loaded and unloaded under saturated conditions (path CDE). Each loading step was maintained for 1 day before the application of the next load increment. The flooding stage lasted 1000 min. Three different liquids were used: distilled water, a saturated solution of NaCl (36g / 100g H_2O at 30°C) and a saturated solution of $Ca(NO_3)_2{\cdot}4H_2O$ (156g / 100g H_2O at 30°C). Total suction ψ –associated with the water potential and equivalent to the osmotic suction on saturation- was used as the relevant variable to assess the action of water with different compositions, which corresponded to $\psi = 0$ (equivalent to a relative humidity of 100%) for the distilled water, $\psi = 39$ MPa (relative humidity of 75%) for the NaCl solution, and $\psi = 92$ MPa (relative humidity of 51%) for the remaining solution.

In a second stage of the experimental programme, a pore fluid replacement test was performed at a constant vertical stress of 1.8 MPa. The sample equilibrated at hygroscopic humidity (relative humidity of around 50% and associated with ψ = 100 MPa) was initially flooded with saturated $Ca(NO_3)_2{\cdot}4H_2O$ solution (ψ = 92 MPa) at a vertical stress of 0.1 MPa. Afterwards, the saturated sample was loaded in steps to the target stress level (path A'B' in Figure 3), in which the intervoid saline fluid is replaced with distilled water (path B'C' in Figure 3). The loading and fluid replacement steps were maintained for 1 day. Finally, the sample was unloaded under saturated conditions with distilled water (path C'D').

A series of splitting tensile strength tests were also included in the experimental programme. These fundamental tests were specifically aimed at studying the micromechanics of grain fracture at different water potentials and time intervals, and corroborate the findings observed at macroscopic deformational scale. Diametral compression tests between flat platens were performed on 30-mm particles that were left under pressure in contact with the three liquids for different time intervals. At the beginning of the tests, the particles were equilibrated at a relative humidity of around 50% (associated with a total suction of 100 MPa). Two series of tests were followed to study the effect of time: a) compression tests on particles that were left for 6 hours under null pressure and b) compression tests on particles that were left under 0.9 MPa for 96 hours. Diametral compression tests were performed under a constant displacement rate of 1.5 mm/hour. Failure of quasi-spherical particles under compression is assumed to be a tensile failure (McDowell & Bolton, 1998). The load-deflection plots presented initial peaks, which corresponded to the fracturing of asperities at contact points. These initial peaks were followed by a large peak corresponding to the maximum load before the catastrophic failure occurred as the particle splits. Splitting tensile strength σ_f was calculated, following McDowell & Bolton (1998), as

$$\sigma_f = \frac{F_f}{d^2} \qquad (1)$$

where F_f is the diametral force corresponding to particle splitting, and *d* the average particle size.

3 TEST RESULTS AND INTERPRETATIONS

Figure 1 shows plots of volumetric strain against vertical stress for the three oedometer tests with sample flooding at 0.9 MPa. The stress-strain curves correspond to constant time intervals of 1000 min. As observed, saturated rockfill is more compressible than dry rockfill, and collapse strains (volumetric compression) develop if the specimen is flooded under load. For the time interval considered, these collapse strains appear not to be affected by the different liquids. However, the compressibility after saturation depends on the total suction (or osmotic suction) of the liquid environment. A higher compressibility on loading is detected at lower total suctions. These findings are in agreement with previous results reported by Oldecop & Alonso (2001), in which these phenomena are controlled by the relative humidity of the air filling the rockfill voids.

As observed in Figure 1, liquid-induced phenomena leading to particle breakage in the vicinity of highly stressed contacts and the subsequent rearrangement of the granular skeleton are more important when distilled water is added. On the other hand, the saline solutions with higher osmotic suctions restrict the passage of the liquid to the rock pores. In this way, a lower damage is induced, which is detected by the lower compressibility on loading. It is admitted that saline solutions present the same osmotic suction assigned to the liquids based on relative humidity considerations. Thermodynamic equilibrium implies that both gaseous environment and liquid environment will have equal chemical potentials, and hence they would produce an equivalent effect on the particle breakage mechanism (Wiederhorn *et al.*, 1982). Freiman (1984) also observed that measured values of crack propagation velocity in liquid environment were proportional to the relative humidity of the gas in equilibrium with the solution. Higher values of osmotic suctions will restrict the passage of water to the rock particles; in the same way as lower values of relative humidity will induce lower water absorption.

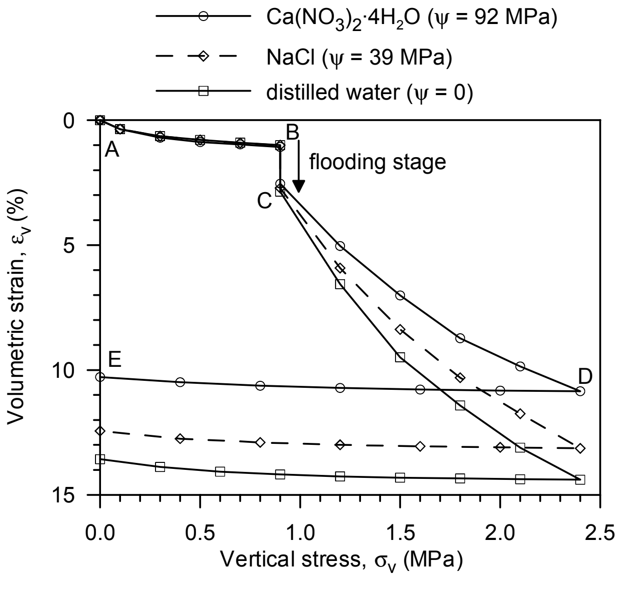

Figure 1. One-dimensional compression tests on rockfill. Specimen flooding at 0.9 MPa (BC). Loading / unloading under saturated conditions (CDE).

Figure 2 shows the time evolution of collapse strains on flooding at 0.9 MPa with liquids of lower total suctions (distilled water and NaCl solution). When liquid was injected, an initial collapse was observed immediately after inundation. At a second stage, however, when the rockfill voids were already saturated, additional collapse deformations were registered with a secondary compression phenomenon developing after a plateau and at elapsed times larger than 100 min. A higher strain rate of this secondary compression was observed when the material was flooded with distilled water.

The behavior observed in Figure 2 can be interpreted as follows. When wetting was induced, the liquid immediately flows through the rockfill voids, filling the macrostructural level and leading to the initial collapse. This phenomenon is probably associated with the instantaneous drop of the matric suction and the loss of stability of the network of grains due to the damage of the particle asperities. Immediately after, a water exchange between the large interparticle voids and the rock particles starts, which continues until equilibrium is reached. This explanation implicitly assumes that two different water potential exist, at a given time, inside the specimen. The water filling the rockfill voids has a macro potential, not necessarily in equilibrium with the water potential inside the particles. Equilibrium will be reached when both water potentials become equal. This hypothesis of liquid transfer and the progressive filling of rock pores can explain the time dependent collapse or secondary compression.

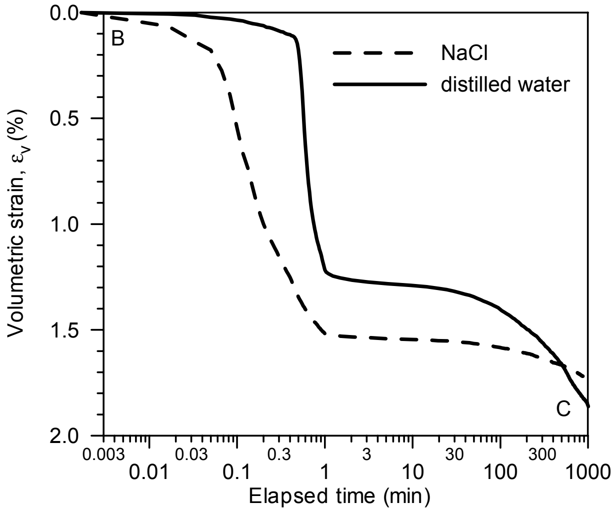

Figure 2. Time evolution of collapse strains on flooding at 0.9 MPa.

Figure 3 shows vertical stress against measured volumetric strain for the flooding test with $Ca(NO_3)_2{\cdot}4H_2O$ at 1.8 MPa. The results of the flooding test at 0.9 MPa (shown in Figure 1) has also been plotted for reference. The magnitude of collapse strains is such that, after flooding at 1.8 MPa, the behavior of the collapsed specimen reaches the normal compression line of the material previously flooded at 0.9 MPa. These results are in agreement with tests on rockfill-type material reported by Oldecop & Alonso (2001), in which the air relative humidity was controlled. In these tests it was found that bringing the relative humidity to 100% leads to a collapse strain equal to that observed in flooded specimens.

Figure 3 also presents the stress-strain results of the pore fluid replacement test that was carried out at a vertical stress of 1.8 MPa (path B'C'). The aim of this test was to study the effect of total suction in liquid environment on the stress path dependency characteristics of specimen deformation. Figure 4 shows the time evolution of volumetric strain undergone by the material on pore fluid replacement, in which the interstitial saline fluid was replaced with distilled water. A quasi-instantaneous compression is detected on total suction decrease, followed by an important time-dependent behavior, which again develops at elapsed times higher than 100 min. A similar response is detected when comparing Figures 2 and 4. Particle breakage on highly stressed contacts is induced as water is progressively incorporated inside the rockfill particles, driven by the difference in the chemical potential between the rockfill voids and the particle pores. The pore fluid replacement test tends to reach the normal compression curve of the material flooded with distilled water at 0.9 MPa and plotted in Figure 1. However, there is still a gap in the compressive strain development that can be explained in terms of the time that the material has been in contact with distilled water. In the case of the pore fluid replacement test, distilled water was in contact with the material for 1300 min, whereas in the flooding test at 0.9 MPa and further loaded to 1.8 MPa the imbibition period was 5200 min.

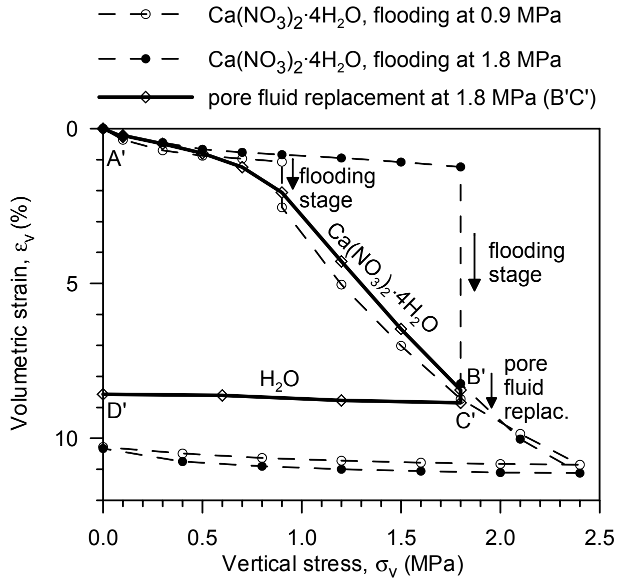

Figure 3. Vertical stress against measured volumetric strain. Flooding tests with $Ca(NO_3)_2{\cdot}4H_2O$ at 0.9 and 1.8 MPa. Pore fluid replacement test at 1.8 MPa.

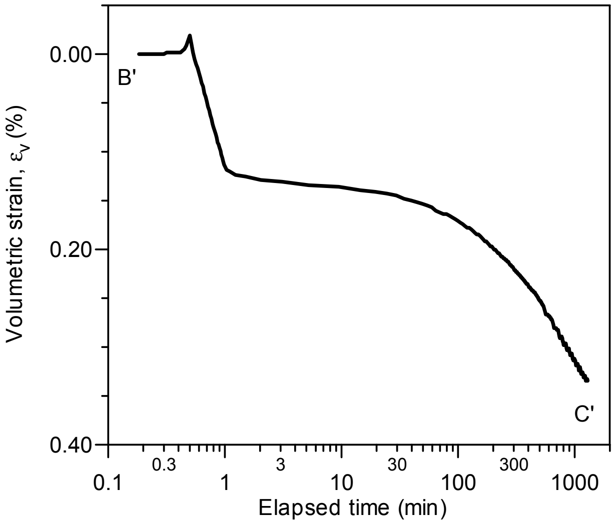

Figure 4. Time evolution of compression strains on pore fluid replacement with distilled water at 1.8 MPa.

Figure 5 shows the particle size distribution curves for different conditions: as-compacted state and as-dismantled states after the execution of the flooding test with $Ca(NO_3)_2{\cdot}4H_2O$ at 0.9 MPa and the pore fluid replacement test at 1.8 MPa. The curves clearly provide evidence of particle breakage due to the increase in the finer fractions. As observed, the material flooded and loaded to 2.4 MPa underwent more crushing of particles.

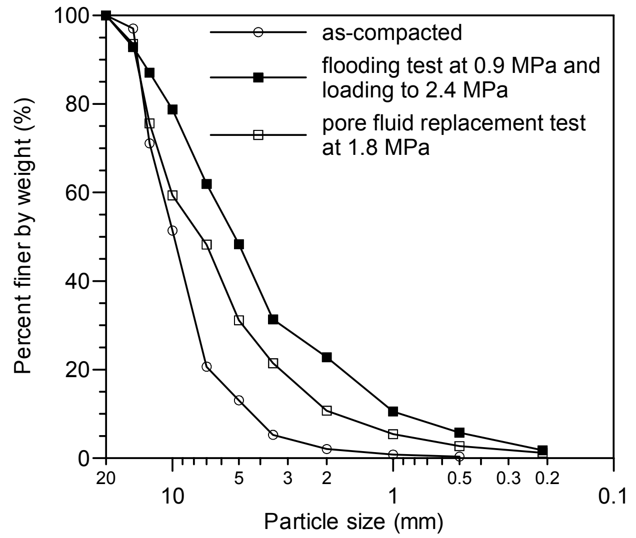

Figure 5. Grain size distribution curves of the tested material. As-compacted state, as-dismantled states (after the execution of the flooding test with $Ca(NO_3)_2{\cdot}4H_2O$ at 0.9 MPa and the pore fluid replacement test at 1.8 MPa).

Results from splitting tensile strength tests (diametral compression tests on particles between flat platens) with different imbibition liquids and periods are shown in Figure 6. The different testing periods in contact with the liquid allowed analyzing the non-local effects on suction equalization. Tests results also included data with particles equilibrated at a constant relative humidity of around 50% (associated with a total suction of 100 MPa), which was the initial suction. After imbibition, a liquid exchange between the boundary condition applied and the dry particles starts. The initial total suction of the particles decreased in search of the boundary condition imposed by the lower suction of the liquid environment. A good consistency in the results is observed when comparing splitting strength results in liquid environment for 6 hours immersion and the results with the initial relative humidity. In this case, a lower damage is induced and a larger splitting tensile strength is detected compared to the long term immersion. Splitting tests on core specimens 84-mm in diameter and 50 mm high performed at different water potentials controlled by relative humidity and reported by Oldecop (2000), were also included for comparison. A somewhat lower value is expected for the larger specimens, as suggested by McDowell & Bolton (1998). These findings regarding the variation of tensile strength with total suction were in agreement with previous results reported by Oldecop & Alonso (2001, 2003), in which these phenomena were controlled by the relative humidity of the air filling the rockfill voids.

4 SUMMARY AND CONCLUSIONS

Results of oedometer tests on a rockfill-type material were presented to study the effect of water composition on material deformational response. Test results showed that the compressibility on loading after saturation with different liquids depended on the water potential of the liquid environment. A significant finding was that bringing the saturated material to a lower water potential by the replacement of the interparticle fluid resulted in an additional collapse. Total suction (relative humidity of the gas in equilibrium with the solution) or, equivalently, osmotic suction of the liquid environment was used as the relevant variable to measure the influence of the liquid action. Time effects were interpreted assuming the existence of two locally different water potentials. A local transfer of water between both levels (interparticle voids and rock pores) explained the nature of observed phenomena. Splitting tensile strength tests were also performed to relate the micromechanics of particle fracture to the deformational behavior observed at macroscopic scale. The diametral compression tests on grains confirmed that particle breakage and crack propagation were controlled by the osmotic suction of the liquid environment and the imbibition period.

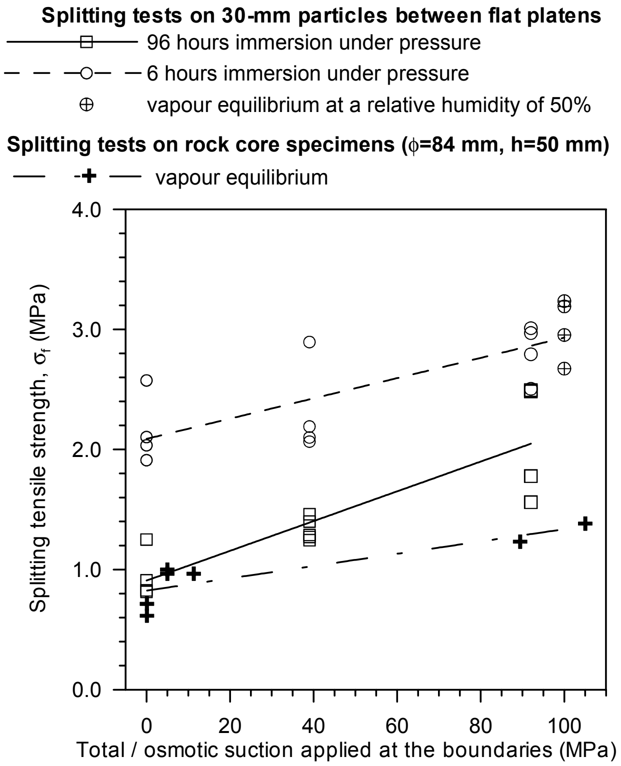

Figure 6. Splitting tensile strength tests. Total suction effects in liquid environment and relative humidity control.

ACKNOWLEDGEMENTS

The authors acknowledge the contribution of Foteini Boiga to the experimental work reported in the paper. Foteini Boiga was recipient of an Erasmus student-exchange scholarship (University of Glasgow).

REFERENCES

Chávez, C. & Alonso, E.E. (2003). A constitutive model for crushed aggregates which includes suction effects. *Soils and Foundations*, 43(4): 215-227.

Coussy, O. (1995). *Mechanics of porous continua.* John Wiley & Sons Ltd. Chichester.

Freiman, S.W. (1984). Effects of chemical environments on slow crack growth in glasses and ceramics. *J. Geophys. Research*, 89(B6): 4072-4076.

McDowell, G. R. and Bolton, M. D. (1998). On the micromechanics of crushable aggregates. *Géotechnique*, 48(5): 667-679.

Oldecop, L.A. (2000). *Compresibilidad de escolleras. Influencia de la humedad.* Doctoral Thesis, Universitat Politècnica de Catalunya.

Oldecop, L. A. and Alonso, E. E. (2001). A model for rockfill compressibility. *Géotechnique*, 51(2): 127-139.

Oldecop, L. A. and Alonso, E. E. (2003). Suction effects on rockfill compressibility. *Géotechnique*, 53(2): 289-292.

Wiederhorn, S.M., Freiman, S.W., Fuller, E.R. and Simmons, C.J. (1982). Effects of water and other dielectrics on crack growth. *J. Mater. Sci.*, 17: 3460-3478.